

Keeping turbofans cool: Aerodynamic upgrade of bypass surface heat exchangers (EU Project SACOC)

*Alberto BROATCH**, *Pablo OLMEDA**, *Jorge GARCÍA-TÍSCAR*[†]* and *Andrés FELGUEROSO**

** CMT–Motores Térmicos, Universitat Politècnica de València
Camino de Vera s/n, 46022 Valencia, Spain*

abroatch@mot.upv.es · pabolgon@mot.upv.es · jorgarti@mot.upv.es · anfelrod@mot.upv.es

[†]Corresponding author

Abstract

New generation turbofan aeroengines are facing a challenge regarding thermal management, and hence, heat exchangers are becoming a key factor in their development. In this context, the EU-funded Clean Sky 2 project SACOC⁵ addressed the aerodynamic upgrade of finned heat exchangers mounted on the inner wall of the secondary duct (bypass) of a turbofan. Such a design implies a significant trade-off between the heat exchanger's thermal performance improvement and the aerodynamic penalties, which are measured by drag or pressure loss. In addition, vibration and noise generation are also of concern, and thus the fluid-structure interaction must be investigated. However, in the case of large turbofan aero engines, full-scale tests are time-consuming and expensive; thus, reduced-scale testing in wind tunnels is much preferable. There are different approaches to designing these reduced-scale wind tunnels, such as a very narrow channel⁸ or, in the case of heat exchangers situated before the outlet guide vanes, a twisted wind tunnel.^{10,13} In this work, we present a summary of a new, cost-effective, reduced-scale wind tunnel design that reproduces turbofan bypass conditions.³ Then we focus on aerothermal and vibration results obtained during the experimental campaign of project SACOC, comprising a baseline standard heat exchanger design and two aerodynamically-upgraded heat exchanger geometry proposals.

1. Introduction

The new generation of aircraft engines, such as ultra-high bypass turbofans or open-rotor concepts, which rely on a gearbox to optimize the rotation speed of the propulsive fans with that of the low-pressure turbine, is facing a serious challenge regarding its thermal management and, hence, heat exchangers are becoming a key factor in their development. The efficiency of these thermal devices is determined by their ability to release the most heat while causing the least pressure loss to the flow. Additionally, it is also desirable to reduce their impact on noise emissions, and thus the fluid-structure interaction must also be studied.

In this regard, an investigation of the aerothermal performance of heat exchangers mounted on the inner wall of the secondary duct of a turbofan is of great interest. To extend the contact wet surface, longitudinal fins can be added to the system to boost thermal performance. The increase of the contact surface will increase the heat exchange but will subject the system to a greater pressure loss and increased aerodynamic perturbations, and thus this trade-off must be carefully assessed. Fig. 1 shows a typical configuration of a SACOC with fins surrounding the outer wall of the secondary duct in a turbofan. Compared with other types of heat exchangers, such as plate/tube ones, this arrangement generates fewer aerodynamic disturbances. If no fins are added to the heat exchanger, the measured mean total pressure losses may decrease in the order of 1%, but a considerably larger decrease in heat exchange is also observed.¹⁰

However, literature on turbofans' thermal management devices is rather scarce due to the general confidentiality of these topics, since it represents a key factor for manufacturers. On the other side, the complexity of reproducing realistic operational conditions and the costs associated with engine tests make this topic rare in public research.

In the Clean Sky 2 project SACOC, we developed a robust experimental methodology which enables a better understanding of the coupled aerothermal processes that occur in these devices. The design of a specific facility to perform the studies with the possibility of tailoring the air velocity distribution around the heat exchanger, together with measurement procedures to capture relevant features of the cooling system are presented. The consortium created for this project was composed of Safran Aircraft Engines, as Topic Manager, Universitat Politècnica de València (UPV), acting as Coordinator, Universidad Politécnica de Madrid (UPM) and Purdue University.

KEEPING TURBOFANS COOL: AERODYNAMIC UPGRADE OF BYPASS SURFACE HEAT EXCHANGERS

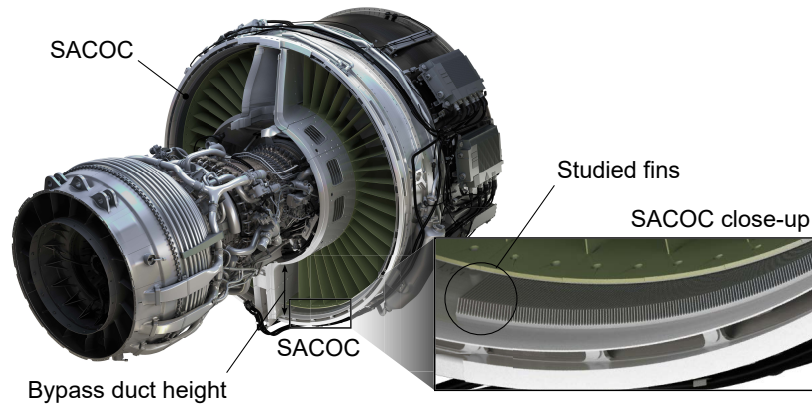


Figure 1: CFM Leap-1A turbfan engine, which employs a SACOC with parallel fins around the outer wall of the bypass duct. The fins studied in this work are highlighted. *Image courtesy of Safran Aircraft Engines.*

2. Experimental setup

2.1 Facility & cost-effective, reduced-scale wind tunnel

In order to achieve similar airflow conditions to those typically found in turbfans, the High Mass-flow and High Temperature (HMHT) gas stand available at UPV is used to supply airflow to a scaled tunnel with a square test section. The wind tunnel includes a settling chamber that dampens and reduces the turbulence created in the previous circuit through a series of honeycombs, a transition to the test section, which features the heat exchanger, and a straight duct which discharges to the ambient. An oil conditioning system in the test room allows full control of the oil circuit and configuring the desired oil mass flow and temperature for the heat exchanger.

Our wind tunnel's core concept is reducing the actual bypass's height and width to a small square section around the SACOC. In order to properly reproduce the bypass flow conditions, i.e. the velocity profile, a custom distortion panel was designed² and installed upstream the test section. It is essentially a 3D-printed screen with varying porosity that causes a certain pressure drop based on that porosity. Three measurement sections have been defined to characterise aerodynamically and thermally the SACOC performance: UMS1, DMS1 and DMS2, which stand for Upstream Measurement Section 1 and Downstream Measurement Section 1 & 2. The conceptual design of the reduced-scale wind tunnel is seen in Fig. 2.

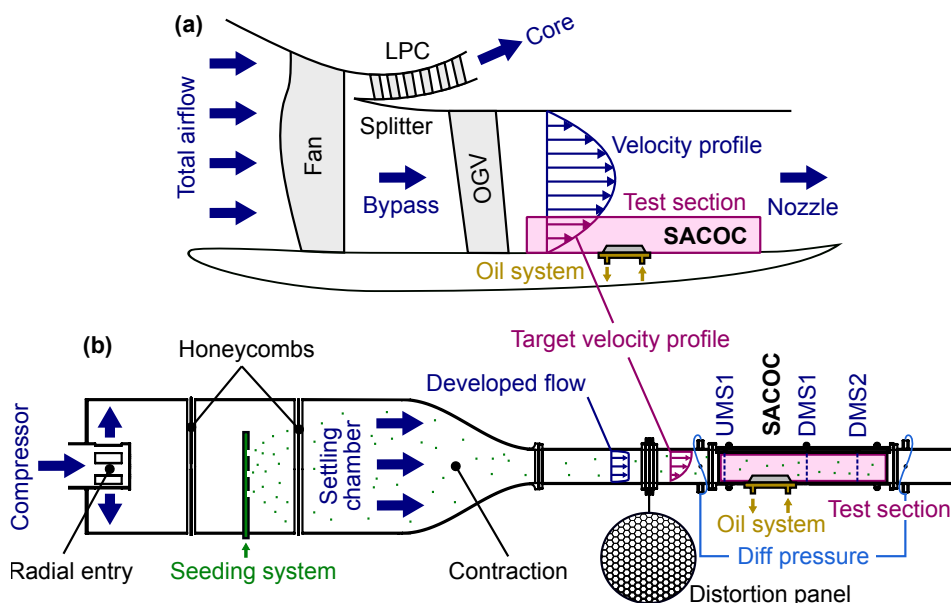


Figure 2: Conceptual design of the reduced-size wind tunnel built for project SACOC.

2.2 SACOC geometries

Four different SACOC geometries were considered in the project. They can be seen in Fig. 3.

- **Baseline:** to establish the baseline for the experimental setup with regard to pressure drop and heat transfer, a flat plate heat exchanger geometry has been first examined. This makes it possible to evaluate the performance of the finned SACOCs more clearly against a reference.
- **Standard:** the air side of the design is given a set of isosceles trapezoidal fins in the second iteration. In order to enhance the surface area in contact with the air and improve convective heat exchange,⁷ it is equipped with a total of 16 fins, each measuring $10^{-2} H$ and $0.2 H$ in width and height, with H being the channel height. This form was chosen because it is typical of modern turbofan SACOCs.
- **Optimized:** in a previous study,⁴ the geometric design of the fin shape on the XY plane was optimised computationally using a CFD solver. The procedure used the pressure drop per lateral fin surface area $\Delta p/A_{xy}$ as the objective function and monitored the heat exchanged to keep it as constant as feasible. The optimisation was based on the adjoint method.^{6,9} Maintaining the heat exchange constant criterion was chosen since this property in aircraft engines is an operability specification, and it is not intended to be changed. The pressure drop, however, is a loss worth lowering.
- **Rounded:** the last version of the geometries consists of a modification of the standard fins that presents sharp edges (the same as in the optimised version) where a blend radius determined through a computational study¹ is employed to improve the aerodynamics of the heat exchanger. A parametric study with a periodic single-fin geometry is employed to do so. A similar approach was employed and reported in the optimisation study,⁴ since fewer cells than a complete simulation imply less computing effort.

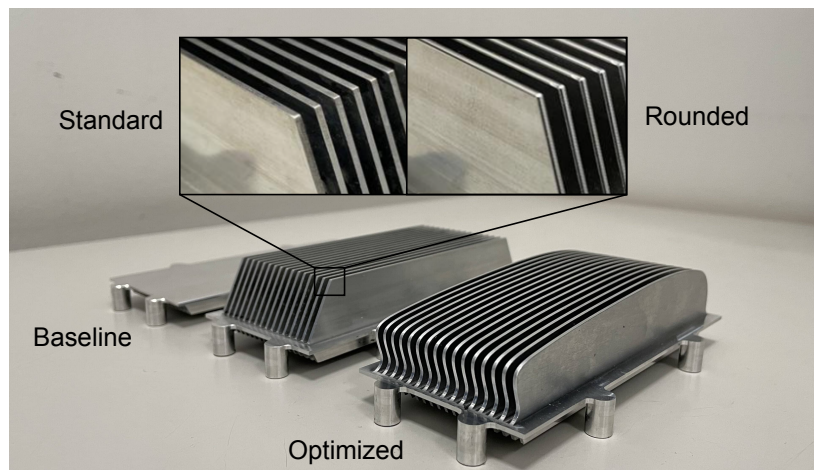


Figure 3: The four geometries considered for the SACOC aerodynamic upgrade.

2.3 Instrumentation

A variety of intrusive and non-intrusive instrumentation was used during the measurement campaign:

- **Kiel probes:** able to measure total pressure and total temperature, mounted on three traverse two-axis systems that enter the test section through upper wall slots at UMS1, DMS1 and DMS2.
- **Differential pressure sensor:** connected through two piezometric rings to pressure taps flush to the wall at the inlet and outlet of the test section, in order to accurately capture the pressure drop of the heat exchanger.
- **Laser-Doppler Anemometry (LDA):** useful to capture time-resolved velocity data at a specific point; it was mounted on a 3-axis gantry to be able to characterize the whole test section.
- **Particle Image Velocimetry (PIV):** both standard 2D PIV and stereoscopic PIV (S-PIV) were used to measure the velocity field at selected planes inside the test section.

KEEPING TURBOFANS COOL: AERODYNAMIC UPGRADE OF BYPASS SURFACE HEAT EXCHANGERS

- **High-speed Schlieren:** taking advantage of the temperature difference of the SACOC wake, this technique was able to characterize the velocity profile downstream of the fins.
- **Thermographic camera:** a long-wave infrared thermographic camera was used to capture the temperature distribution over the surface of the heat exchanger.
- **Laser-Doppler Scanning Vibrometer (LDV):** it was used to capture the Operational Deflection Shapes (ODSs) of the heat exchanger fins during operation.

3. Results & discussion

3.1 Velocity

Despite the fact that the primary function of a heat exchanger is to extract as much heat from the hot source as possible, in this application, it is necessary to do so without significantly affecting the aerodynamics on the air side. This is because the exchanger uses the bypass airflow as a cold sink, but this airstream will then be expanded in the secondary nozzle to produce thrust. Thus, pressure drop and velocity distortion will negatively affect the engine performance.

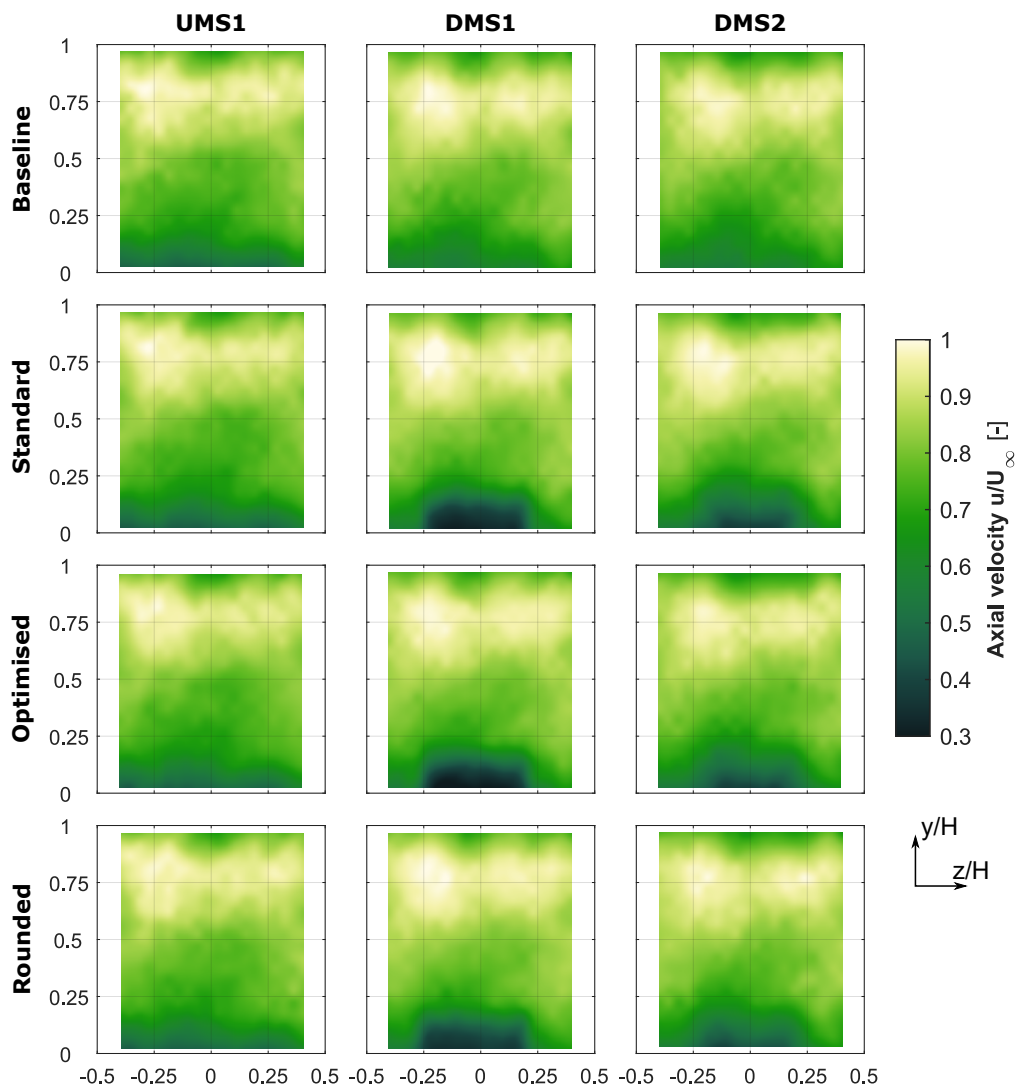


Figure 4: Velocity fields comparison for the different SACOC geometries (rows) measured at UMS1, DMS1 and DMS2 (columns) with a typical measurement uncertainty of ± 0.06 . Note especially the clear "velocity sink" that appears in the wake of the finned versions.

First, using the conventional isentropic flow relations, velocity is calculated from the Kiel total pressure and temperature data as well as the static pressure captured through the piezometric rings. The analysis of interpolated velocity contours is shown in Fig. 4, where each row shows the velocity evolution along the sections for one version and each column reflects the contours in the same section for the various SACOC versions. As expected, the gradients in the velocity field at UMS1 follow the intended profile and displays essentially identical contours in the four versions. The results in the three measurement sections are quite comparable when looking at the baseline geometry, which also somewhat reduces the gradients present in UMS1 in the downstream sections.

The three finned versions exhibit comparable behaviours, with the fins having a significant impact on the velocity at DMS1. In all situations, there is a region towards the bottom with particularly low values and an interface where the conditions become freestream-like. In the case of the optimised fins, this zone appears to be smaller than the standard, but the rounded geometry seems to be even less perturbed. The SACOC fins also have an impact on the downstream-most section, DMS2, but here the area of influence is less well defined than it was in DMS1 and, instead, extends towards the lateral walls and accelerates again. The test section's lateral zones, which are not behind the fins, suffer an acceleration compared to their values in the UMS1 up to a height that is similar to what is seen in the wake. Additionally, the gain in speed is greater in DMS1.

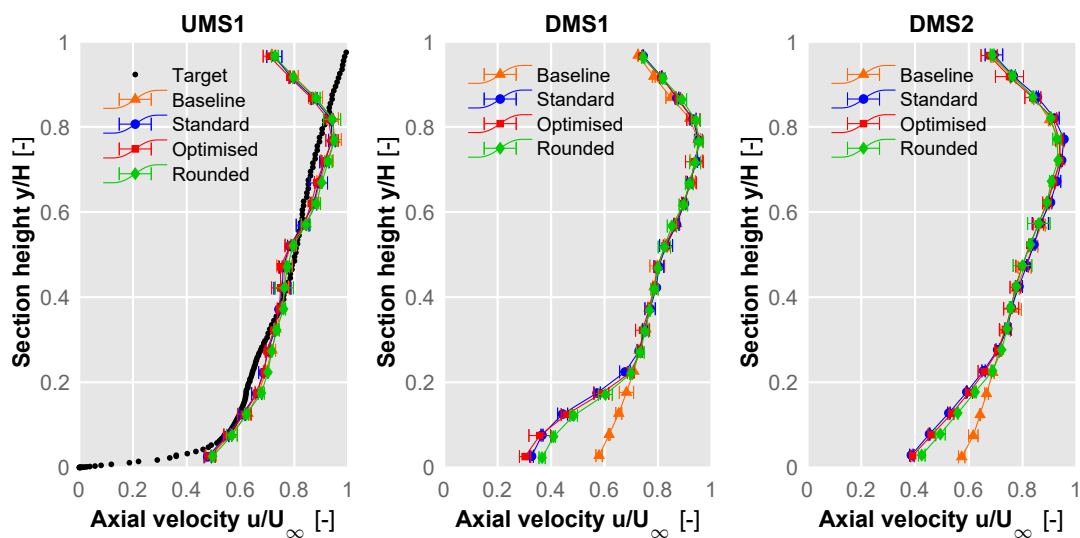


Figure 5: Velocity profiles averaged in the central region of the tunnel, $Z \in (-0.25H, +0.25H)$, for the different geometries at each section with a typical measurement uncertainty of ± 0.06 . Error bars show STD between measurements.

In Fig. 5, velocity profiles are shown for a more thorough study. These are the velocity averaged values of the four different versions for the SACOC span's centre region, $Z \in (-0.25H, +0.25H)$. This averaging is done to prevent solely showing the impact of the specific fin or channel in the centre. The velocity profiles for the UMS1 are nearly identical and very similar to the target velocity profile sought, validating the design of the distortion panel.

There are very slight changes in the baseline model's velocity profile from one plane to another, thereby maintaining the impact of the distortion screen throughout the tunnel test section. The finned geometries, on the other hand, exhibit a clear effect on the downstream planes of lower velocities caused by the SACOC wake, being the deceleration clearer in DMS1 (already seen in Fig. 4). Here, nevertheless, it is possible to observe that the standard and the optimised versions present almost identical values in the whole height, whereas the rounded version has higher values in the wake than the previous ones. Again, this effect is more noticeable in DMS1. This can be explained by the fact that rounding the edges of the fins reduces the aerodynamic impact on their leading edge. This allows the flow to remain attached to the surface, not blocking the channel between consecutive fins, and, thus, reducing the aerodynamic impact.

Another point worth mentioning is that the four versions, despite having different velocities in the wake, present identical values above a height of around 25-30% of the section in the downstream regions. This implies that the fins' influence is confined to an area that is just very little above them. It can be seen that a boundary layer is generated on the top wall of the tunnel above a height of 75% of H (which is absent in the bypass at this height), but it does not interact with the area affected by the SACOC. This supports the idea of a wind tunnel with a limited height can provide relevant results as long as the top is far enough from the fins.

In order to assure the veracity of the results obtained, the first step is to perform a cross-validation. To do so, the velocity profiles along the centerlines of the three measurement sections are compared among the different techniques

KEEPING TURBOFANS COOL: AERODYNAMIC UPGRADE OF BYPASS SURFACE HEAT EXCHANGERS

used, both intrusive and non-intrusive. This comparison is displayed in Figure 6. It includes Kiel probe data, LDA, PIV and stereo-PIV measurements for the three planes, and also Schlieren-based velocimetry at DMS1. Additionally, the desired upstream velocity profile coming from the real engine bypass is plotted at UMS1. On one hand, a good overlap of the results is shown, which is a good indication of their reliability. The experimental velocity profile, on the other hand, is also in good accord with the desired engine target in all cases.

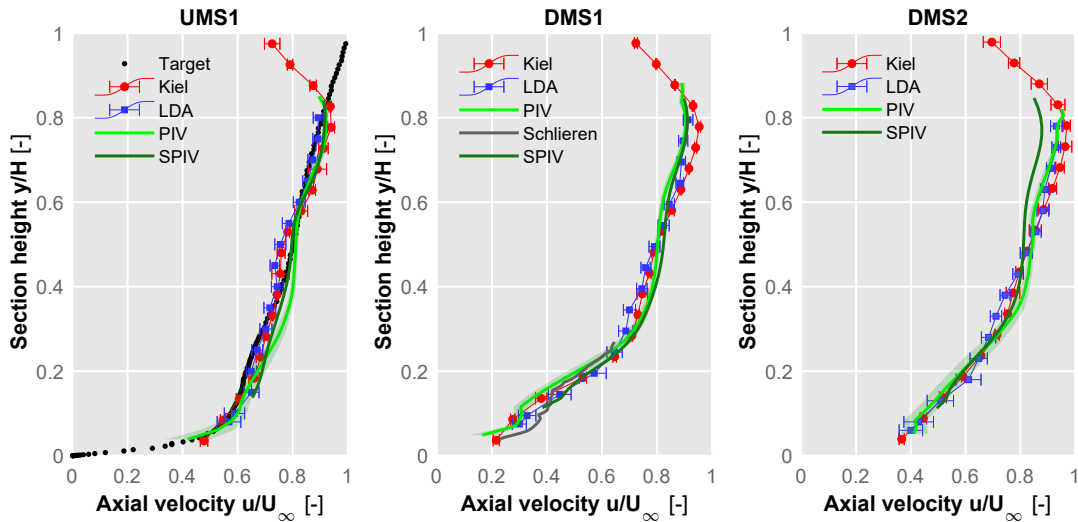


Figure 6: Velocity profiles in the centreline of the three measurement planes measured with Kiel probes (intrusive), LDA, and PIV (both, 2D and stereoscopic). In the lower region of DMS1, also the velocities have been extracted from the Schlieren measurements with PIV techniques. Kiel results averaged between $Z \in (-0.25H, +0.25H)$.

The velocity field measured with the Stereoscopic PIV is shown in Fig. 7 in each of the three measurement planes UMS1, DMS1 and DMS2, showing the three components of the velocity. Although a comparable approach as the standard PIV (i.e. progressively moving the laser sheet) might be used to characterise the entire test section volume, the setup in the case of S-PIV is more complex, relying on a Scheimpflug mounting, and only the three measurement sections have been examined. To appreciate the in-plane components, vectors have been upscaled in the out-of-plane component by 20%. While the S-PIV technique is more expensive and difficult to calibrate, the amount of information obtained in each measurement can justify its implementation.

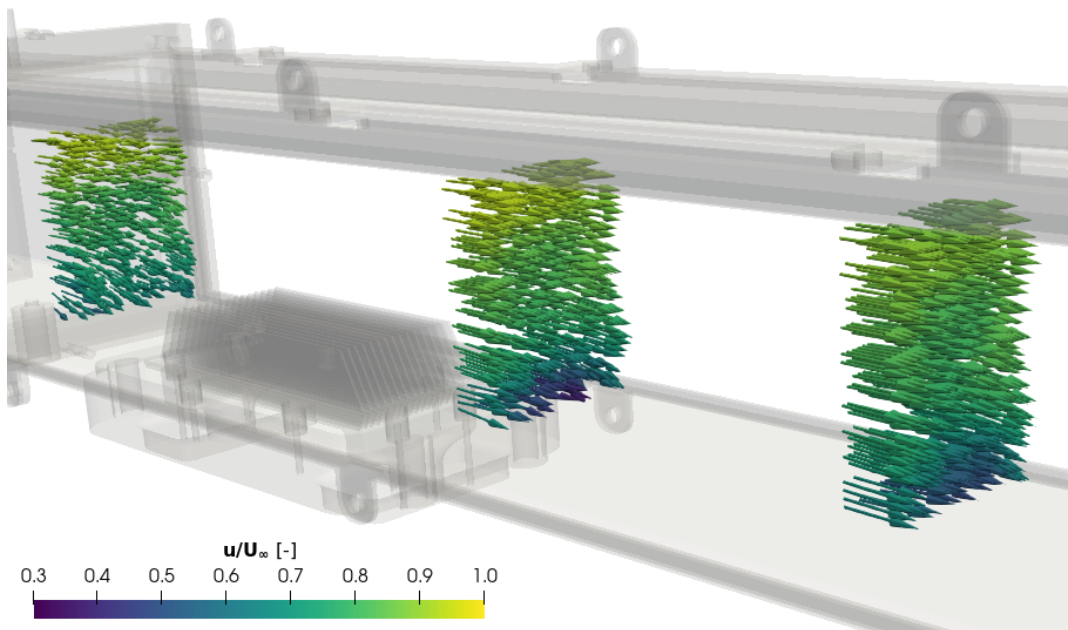


Figure 7: Velocity vectors from S-PIV at the three measurement sections UMS1, DMS1 and DMS2.

3.2 Pressure drop

As explained above, the pressure drop induced in the bypass duct is one of the fundamental metrics of a SACOC device. With regard to the pressure drop caused by the exchanger on the air side, Fig. 8 depicts the pressure drop for each version under various operating conditions, as measured between the test section inlet and outlet piezometric rings. In the case of an incompressible flow, the pressure decrease can be expressed as follows:¹²

$$\Delta p = K \frac{1}{2} \rho V^2 \quad (1)$$

where ρ is the density, V is the velocity magnitude and K is a pressure drop coefficient that only depends on the Reynolds number, but it becomes independent for high enough Re values.¹¹ By recalling the continuity equation $\dot{m} = \rho AV$, this can be rearranged as:

$$\Delta p = \frac{K}{2A^2} \frac{\dot{m}^2}{\rho} \quad (2)$$

The term \dot{m}^2/ρ should therefore be roughly linear for Δp . This is shown true for all four configurations at the considered mass flow range, around $\pm 15\%$ of the nominal flow, as depicted in Fig. 8. The fundamental benefit of this fact is that it allows for easy computation of losses under various air mass flow settings and ensures that the pressure drop for each configuration is defined by a constant K .

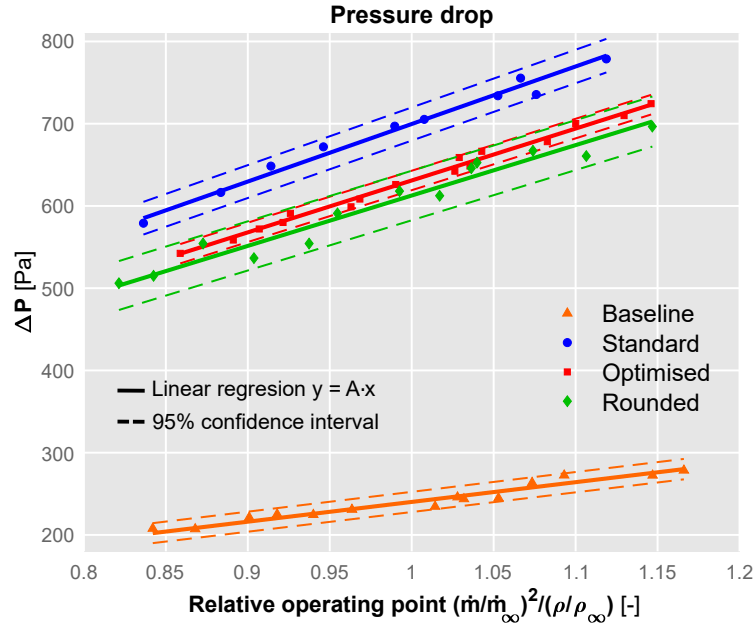


Figure 8: Pressure drop variation between piezometric rings with the relative operating point (nominal conditions = 1) for each geometry with a typical measurement uncertainty of $\pm 1\%$.

As predicted, the flat plate's pressure drop is significantly smaller than the fins' pressure drop. The pressure drop associated with the optimised version of the fins is lower than that of the standard fins, reaching almost a 10% reduction in pressure drop under nominal conditions, supporting the numerical optimisation technique even though they have very comparable velocity distributions. This can be explained by the variations in how both geometries interact aerodynamically with the flow, as thoroughly examined by Chávez et al.⁴ In comparison to the geometry with conventional fins, the optimised geometry exhibits significantly lower turbulent kinetic energy values in the wake and essentially no vortical structures are created on the tip of the fins.

Nonetheless, the performance of the rounded SACOC is remarkably good. Just using a blend radius for the fins' edges reduces the pressure drop in the same order as the topologically optimised shape, presenting even better figures. This can be explained by a more aerodynamically-favorable leading edge of the fins, reducing the boundary layer detachment and therefore, letting the air pass through channels between the fins that are virtually larger (a more abrupt detachment would cause blockage of a larger cross-section). However, rounding the edges increases manufacturing costs, so the trade-off must be evaluated by the designer. Note that in this project, oil-side geometries are not realistic, and thus oil-side pressure drop is not analyzed, as only the aerodynamic upgrade of the SACOC was targeted.

3.3 Fluid-Structure Interaction (FSI)

Besides the analysis of the velocity and pressure drop of the surface heat exchanger, it is interesting to study the interaction that the fins can have with the flow. The vibration of a heat exchanger can be negative in most cases, acting as a source of noise, causing fatigue, crack formation or even increasing turbulence and pressure loss. There may be some positive side effects though as well, such as the enhancement in heat exchange capacity caused by an increment of the heat transfer convective coefficient. Figure 9 illustrates the vibration of the outermost fin, together with its modes. The first mode values are used to normalise frequencies and displacements. The Operational Deflection Shapes (ODSs) are shown together with the frequency and displacement values associated with them.

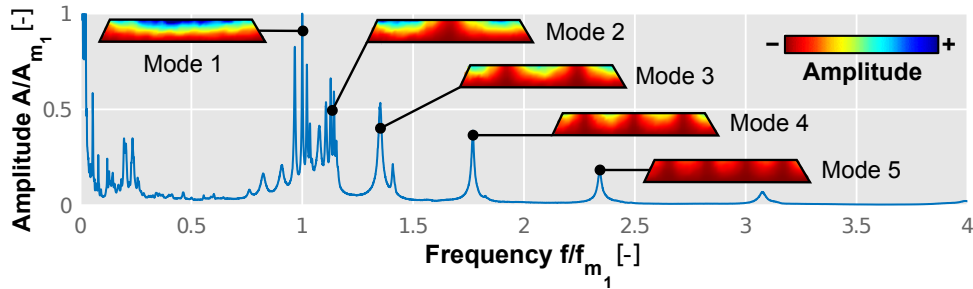


Figure 9: Experimental average vibration spectrum of the outermost fin of the SACOC with Operational Deflection Shapes. Amplitudes and frequencies are rendered dimensionless with the first mode values.

Studying the vibrations with LDV has many benefits, one of which is the ability to study the entire surface without adding any mass. In order to perform a similar evaluation using accelerometers, adding mass to the fin could change not only its structural characteristics but also the outcome due to the altered fluid-structure interaction.

To corroborate the results obtained experimentally, the geometry has been analysed numerically through the Finite Elements Method (FEM) using Ansys Mechanical. The geometry has been discretised into 153 000 tetrahedral

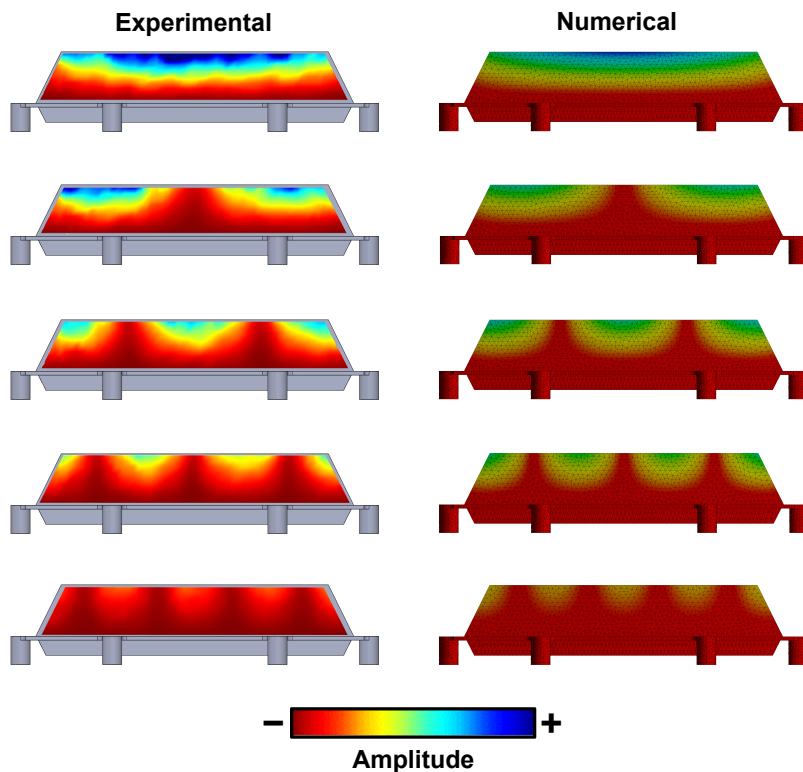


Figure 10: Comparison between the experimental Operational Deflection Shapes and the numerical first 5 principal vibration modes in the outermost fin of the standard geometry.

KEEPING TURBOFANS COOL: AERODYNAMIC UPGRADE OF BYPASS SURFACE HEAT EXCHANGERS

cells. Those parts in contact with the oil pan, i.e., the cylinders used to screw the SACOC to the pan and the lateral faces of the base, have been considered to be fixed. The model has been configured to not be pre-loaded, with a harmonic response and not damped. The first 100 modes are analysed employing the Block Lanczos algorithm, which uses an automated shift technique to extract the desired number of eigenvalues.

Figure 10 represents the comparison of the measured ODSs and the numerically-predicted first five vibration modes. Note that these experimental ODSs do not correspond to the whole heat exchanger, but to those that have been measured on the outermost fin, as is the one which is accessible by the LDV. In the five cases, the deformation of the outermost fin at the specific frequencies presents almost identical behaviours. Table 1 displays the numerical and experimental results together with the relative errors between them. Similar to Fig. 9, the first five modes are examined, normalising the values with the experimental frequency of the first mode, being \bar{f}_{Exp} the normalised experimental frequency and \bar{f}_{Num} the one obtained numerically.

Table 1: Comparison of the normalized frequencies of the first 5 modes between the experimental measurements and the FEM-predicted values and their relative error.

Mode	\bar{f}_{Exp}	\bar{f}_{Num}	ε
1	1	0.999	0.1%
2	1.128	1.129	0.09%
3	1.352	1.389	2.66%
4	1.769	1.803	1.89%
5	2.341	2.370	1.22%

When taking into account the outcomes in Table 1, together with the ODS from Fig. 10, it is reasonable to conclude that for the first five modes, the LDV-captured values agree with the theoretical ones with a deviation lower than 2.66%, verifying the results. The average vibration spectrum of the three finned geometries is displayed in Fig. 11. This analysis can provide a better understanding of the aerodynamic performance of these heat exchangers.

It is possible to observe that the fin displacement of the first four modes is considerably larger in the standard geometry than in the other two, which present similar values of displacement. Furthermore, the spectrum of the standard and the rounded geometry feature their modes almost at the same frequencies, since their geometry is practically identical, whereas the optimised geometry presents similar but slightly different values.

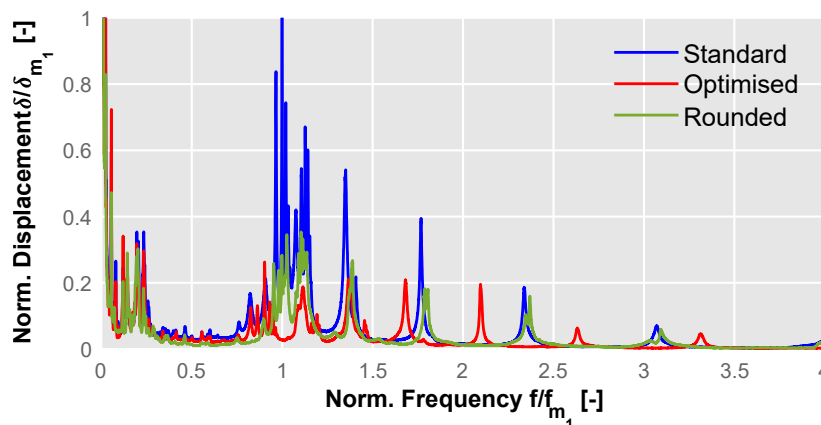


Figure 11: Comparison of the vibration spectrum between the different finned geometries. The normalisation values correspond to those of the standard geometry first mode.

The displacement of these first four modes in the optimised and rounded versions are in the same order of magnitude, around 20–30% of the first mode displacement in the standard case. However, the displacements of the standard geometry decrease until the same values as the other two are reached at the fifth mode and beyond. This behaviour of the finned geometries can be related to their induced pressure drop too. The higher values of displacement in the standard geometry could lead to a more turbulent flow, besides from the possible higher energy absorption that also induces a larger flow pressure loss. In the case of the optimised and rounded geometries, the amplitudes throughout the spectrum are very similar, as was the case of the measured pressure drop discussed before.

3.4 Temperature

Despite the fact that the aerodynamic behaviour of this type of heat exchanger is of great importance, their main purpose is of course cooling down the oil. For this reason, a detailed analysis of the temperature fields and heat exchange is crucial. In general, the thermal specifications of a heat exchanger are fixed for a certain application, i.e., they are used to release a certain amount of heat from a hot source. Therefore, a typical design goal would be to maintain the heat transfer for the different versions and minimize size (and thus, weight) and pressure drop.

However, another study which can be also interesting to compare is to keep the incoming conditions of air and oil mass flows and temperatures and analyse the performance of each version. Hence, even if there are models that exchange more heat, they can be down-scaled to save weight and reduce impact in the air. This is the considered case.

Figure 12 displays temperature contours on the air side obtained from the thermocouples in the Kiel probes. There is a gap in the contours at the bottom because the Kiel thermocouple cannot measure the lower 7.5% of the section. The figure demonstrates that the temperature only rises in the vicinity of the fins, up to a 25–30% of the section, a height which is similar to the velocity wake (see Fig. 4); above that point, the temperature is nearly constant, but the temperature rises as it gets closer to the bottom in the lower part.

Since the most heated portion of the air goes downstream together with the velocity wake, the influence of the fins is not seen close to the lateral walls either. The thermocouples in the probes are unable to measure the baseline temperature increase since it is weaker and restricted to lower locations that they cannot reach. There is a rise in

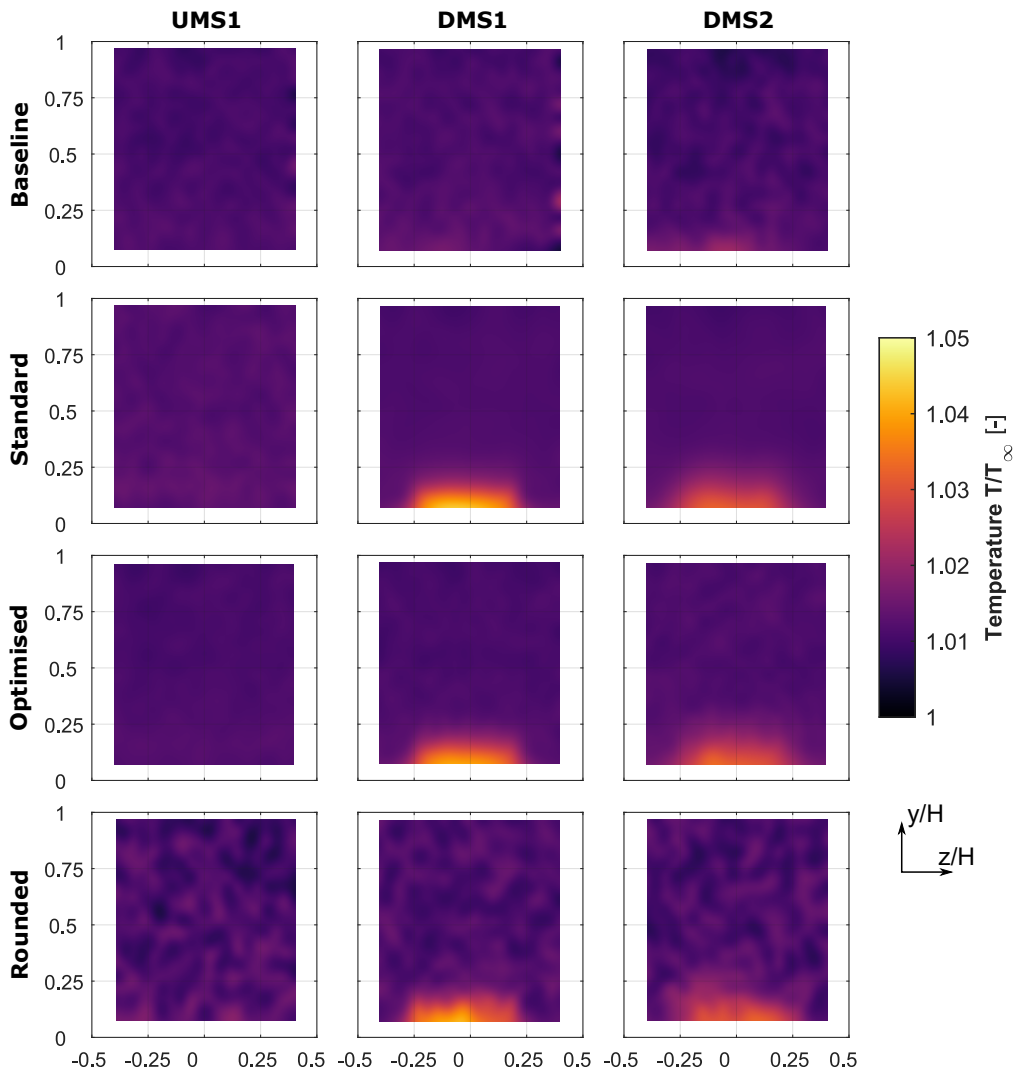


Figure 12: Total temperature fields comparison for the different SACOC geometries (rows) measured at UMS1, DMS1 and DMS2 (columns) with a typical measurement uncertainty of ± 0.004 .

KEEPING TURBOFANS COOL: AERODYNAMIC UPGRADE OF BYPASS SURFACE HEAT EXCHANGERS

temperature that follows the finned pattern for the standard, optimised and rounded versions.

Now that the air has been studied, it is time to move on to the oil section and analyse its temperatures and the heat exchanged. In this case, the heat exchanged by the different SACOC models is determined by carefully examining the oil circuit. Thus, acquiring the oil temperature at the inlet and outlet by means of 8 RTDs and measuring the oil mass flow, assuming constant heat capacity, the heat transfer is defined as:

$$\dot{Q} = \frac{\dot{m}_o C_{p,o}}{4} \left(\sum_{i=1}^4 T_{in_i} - \sum_{i=1}^4 T_{out_i} \right) \quad (3)$$

Since the oil pan is made of an insulating material, it is assumed that, as an approximation, all the extracted heat from the oil is delivered to the air. Under nominal conditions, the mean flow rate is $18.1 \times 10^{-3} \dot{m}_\infty$ on the oil side (where \dot{m}_∞ is the nominal air mass flow), the fluid enters the pan with an average temperature of $1.33 T_\infty$ and moves in a laminar regime below the SACOC. The fluctuation in these values and air conditions from one version to another is less than 1%. The temperature of the oil dropped after exiting the heat exchanger by 1.115% for the baseline, 2.936% for the standard fins, 3.234% for the optimised version and 3.296% in the rounded case. Considering the heat exchanged by the baseline to be \dot{Q}_b , these results lead to a heat evacuation of $2.711 \dot{Q}_b$, $2.895 \dot{Q}_b$ and $3.113 \dot{Q}_b$ for the standard, optimised and rounded geometries, respectively. These results are displayed in Table 2.

Table 2: Heat exchanged by the SACOCs referred to the baseline case under nominal conditions.

Baseline	Standard	Optimised	Rounded
\dot{Q}_b	$2.711 \dot{Q}_b$	$2.895 \dot{Q}_b$	$3.113 \dot{Q}_b$

Finally, after analysing the air and the oil domains, also the solid domain can be characterized from a thermal point of view. To perform this characterisation, infrared thermography is used. The SACOC is imaged using an IR camera from the top side with a window that allows the long-infrared range between 9 and $14 \mu\text{m}$ to get through. Fig. 13 shows the results for each geometry.

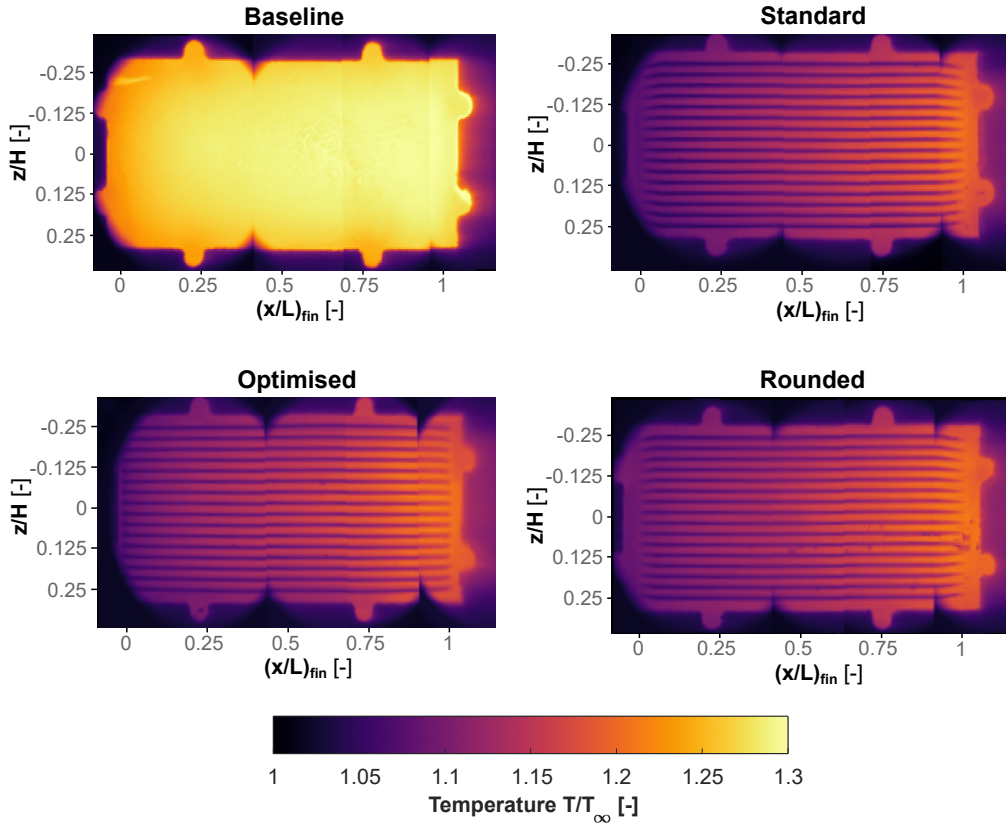


Figure 13: Composite base temperature distribution of the four SACOC geometries.

KEEPING TURBOFANS COOL: AERODYNAMIC UPGRADE OF BYPASS SURFACE HEAT EXCHANGERS

Both the tunnel floor and the heat exchanger were painted black using graphite-based paint in order to provide a uniform emissivity. This emissivity was specifically calibrated using a surface thermocouple for these measurements at the corresponding operating conditions. The Field of View (FoV) of this window does not capture the whole length of the heat exchanger, so different images were acquired and a final image was reconstructed. The same procedure was applied to the rest of the geometries.

One of the most important outcomes that can be derived from Fig. 13 is the difference in temperatures between the baseline and the finned versions. The temperature is not only considerably higher in the baseline case, but it also presents a more uniform distribution than the rest of the models. This can be explained straightforwardly when considering the cooling effect of the fins. Since they enhance the heat exchange, the cooling that occurs in the baseline is much poorer, the temperature, therefore, being higher.

Additionally, as the aluminium presents a very good conductivity, the temperature is quite uniform. The other cases present somewhat more differences in the flow-wise direction because of the higher interaction of the air with the exchanger due to the fins. The temperature distribution of the standard, optimised and rounded geometries are quite alike, presenting higher values in the oil inlet, close to $(x/L)_{fin} = 1$, that decrease to the left (air inlet and oil outlet) and along the centre, $z/H = 0$, that diminish to the lateral of the heat exchanger.

This highlights the importance of optimizing the oil flow distribution on the liquid side of the heat exchanger, and also of taking that oil flow pattern into account if an optimization of the air side geometry is performed. As the potential for heat transfer to the air is different according to the areas where the oil temperatures are higher, this information must be fed to the optimization procedure in order to extract the maximum advantage from it. Ideally, a conjugated heat transfer (CHT) optimization which solves the coupling of the air, solid and fluid domains must be performed to obtain the most advantageous aerodynamic optimization of the SACOC.

4. Conclusions

In this work, a methodology has been presented to thoroughly characterise surface air-cooled oil coolers for turbofans experimentally, together with the aerothermal results obtained during operating conditions of these types of heat exchangers. Table 3 provides a summary of the findings for pressure drop and heat transfer in the form of the Fanning friction factor f (derived from the data presented in Fig. 8) and the overall heat transfer coefficient U (derived from the data presented in Table 2).

Table 3: Summary of the aerothermal performances of the four geometries as Fanning friction factor f and overall heat transfer coefficient U .

Geometry	$f \times 10^3$ [-]	U [W/(m ² K)]
Baseline	11.18	314.08
Standard	32.52	896.02
Optimised	29.33	942.88
Rounded	28.48	1073.28

Although adding fins to a typical flat plate design increases significantly the amount of heat exchanged, the pressure drop caused in the air side also increases. However, it has been shown that a topologically optimised design, achieved by numerical simulations, can yield a considerable reduction in pressure drop and an increase in heat exchange compared to conventional fins. This effect is even more notorious in the model with rounded fins. In fact, the two last cases improve the heat transfer more than they worsen the pressure loss when compared to the baseline, something that does not happen with the standard geometry.

Regarding the finned heat exchangers, the f factor has been reduced by 9.8% when optimising the shape of the standard fins, and even the small modification of rounding its edges can improve by 12.42% this factor. Something similar occurs with the overall heat transfer coefficient, which rises by 5.2% in the optimised model and almost 20% in the rounded one. This puts into manifest the importance of a careful design or selection of the heat exchanger for a particular operation.

Therefore, the main conclusions derived from the research done in this work can be summarised as follows:

- By applying different measurement techniques, the methodology has been shown to be robust and reliable since the veracity of the results could be cross-validated using different approaches. The proposed techniques provide overlapping and complementary information, which enhances the understanding of the heat exchanger performances and increases confidence in the outcomes obtained.

KEEPING TURBOFANS COOL: AERODYNAMIC UPGRADE OF BYPASS SURFACE HEAT EXCHANGERS

- When performing experimental characterisations in small-scale wind tunnels at high speeds, optical techniques should always be considered, not only for their versatility but to ensure that the measurement instruments such as probes, thermocouples, accelerometers, etc. do not impact the actual performances of the studied model.
- The impact of four heat exchangers with different geometries has been analysed: a flat plate (baseline), a heat exchanger with standard trapezoidal fins (standard), one with topologically optimised fins (optimised) and another finned one with the standard geometry but with its edges have been rounded (rounded). The addition of fins to the baseline increases considerably both pressure drop and heat exchange. However, a careful optimisation of the fins' geometry can yield increases in heat exchange and reductions in pressure losses. Furthermore, considering the very high Reynolds and compressible Mach regime of the operating conditions, rounding the edges of the standard geometry improves the heat exchange and gets better results in pressure drop. It is highly significant because, comparing the rounded geometry outcomes with those from the baseline, the increase in heat exchange is higher than the pressure loss produced by the fins.
- The possibility of characterising surface heat exchangers for turbofans in this type of reduced-scale wind tunnel has been demonstrated. As long as there is enough space between the heat exchanger and the surrounding walls, the effects related to the SACOC are confined to a region not much larger than its own size downstream of it. In this case, being the fins height the 20% of the tunnel's, the aerothermal effects were observed below the 30% of the test section height. In the width-wise direction, the effects were in the same order. This kind of reduced-size facilities thus allows testing full-sized SACOC fins at realistic engine take-off conditions, reducing the necessity of full engine tests which are greatly expensive and very time-restricted, and facilitating the development of the advanced thermal management solutions that the next generation of aeroengines requires in order to enable a more sustainable air transport.

5. Acknowledgments

This project has received funding from the Clean Sky 2 Joint Undertaking under the European Union's Horizon 2020 research and innovation programme under grant agreement n° 831977: *Aerodynamic upgrade of Surface Air-Cooled Oil Coolers (SACOC)*.

References

- [1] A. Broatch, J. García-Tíscar, A. Felgueroso, M. Chávez-Modena, L.M. González, and E. Valero. Numerical and experimental analysis of rounded fins for high speed air-cooled heat exchangers. *International Journal of Heat and Mass Transfer*, 201:123575, 2023.
- [2] A. Broatch, X. Margot, J. García-Tíscar, and A. Felgueroso. An automatized methodology to generate velocity distortion panels for wind tunnel testing. *Journal of Wind Engineering and Industrial Aerodynamics*, 227:105065, 8 2022.
- [3] A. Broatch, P. Olmeda, J. García-Tíscar, A. Felgueroso, M. Chávez-Modena, L.M. González, M. Gelain, and A. Couilleaux. Experimental aerothermal characterization of surface air-cooled oil coolers for turbofan engines. *International Journal of Heat and Mass Transfer*, 190:122775, 7 2022.
- [4] Miguel Chávez-Modena, Leo Miguel González, and Eusebio Valero. Numerical optimization of the fin shape experiments of a heat conjugate problem surface air/oil heat exchanger (SACOC). *Journal of Heat and Mass Transfer*, 182:121971, 2021.
- [5] European Commission. Aerodynamic upgrade of surface air cooled oil cooler (SACOC). <https://cordis.europa.eu/project/id/831977>. [Accessed 03-Jul-2023].
- [6] Flavio Giannetti and Paolo Luchini. Structural sensitivity of the first instability of the cylinder wake. *Journal of Fluid Mechanics*, 581(1):167–197, 2007.
- [7] Frank P. Incropera. *Fundamentals of heat and mass transfer*. John Wiley, Hoboken, NJ, 6th ed edition, 2007.
- [8] Sangkeun Kim, June Kee Min, Man Yeong Ha, and Changmin Son. Investigation of high-speed bypass effect on the performance of the surface air–oil heat exchanger for an aero engine. 77:321–334.
- [9] Paolo Luchini and Alessandro Bottaro. Adjoint equations in stability analysis. *Annual Review of fluid mechanics*, 46:493–517, 2014.

KEEPING TURBOFANS COOL: AERODYNAMIC UPGRADE OF BYPASS SURFACE HEAT EXCHANGERS

- [10] J. Sousa, L. Villafañe, and G. Paniagua. Thermal analysis and modeling of surface heat exchangers operating in the transonic regime. *Energy*, 64:961–969, 2014.
- [11] Philip Thomas. *Steady-state compressible and incompressible flow*, chapter 4 & 6, pages 32–40 & 50–59. Elsevier, first edition edition, 1999.
- [12] AJ Torregrosa, A Broatch, J García-Tíscar, and F Roig. Experimental verification of hydrodynamic similarity in hot flows. *Experimental Thermal and Fluid Science*, 119:110220, 2020.
- [13] Laura Villafañe and Guillermo Paniagua. Aerodynamic impact of finned heat exchangers on transonic flows. 97:223–236.